Electronic Supplementary Material (ESI) for Journal of Materials Chemistry A.

Supplementary Information for

Layered 2D Alkyldiammonium Lead Iodide Perovskites: Synthesis, Characterization, and Use in Solar Cells

Majid Safdari[a], Per H. Svensson[a,c], Minh Tam Hoang[b], Ilwhan Oh[b], Lars Kloo[a] and James M. Gardner[a]

[a] Division of Applied Physical Chemistry, Department of Chemistry, KTH Royal Institute of Technology, SE-100 44, Stockholm, Sweden.

[b] Department of Applied Chemistry, Kumoh National Institute of Technology, Gumi, Gyeongbuk, Korea

[c] SP Process Development, Forskargatan, 15121 Södertälje, Sweden

Table S1. Bond length and angles in the $BdPbI_4$, $HdPbI_4$ and $OdPbI_4$ compared with $MAPbI_3$

	$BdPbI_4$	$HdPbI_4$	$OdPbI_4$	$MAPbI_3$
Distance between 2Pb in 2 different planes(Å)	10.383	11.845 Å	13.737Å	6.284
Distance between 2Pb in the same planes(Å)	6.101	6.190	6.138	6.284
Pb-I bonds in the plane(Å)	3.205 3.183 3.170 3.211 3.181 3.186	3.220 3.213 3.180	3.202 3.187 3.192	3.142
Pb-I-Pb	149.87	148.31	147.44	180

Table S2. Atomic parameters for OdI_4 obtained from single crystallography characterization.

Atom	Ox.	Wyck.	Site	S.O.F.	x/a	y/b	z/c	U [Å^2]
Pb1		2d	-1		1/2	1/2	1.00000	
I1		4e	1		0.45589(4)	0.19045(5)	0.78278(5)	
I2		4e	1		0.26297(4)	0.57228(6)	0.87052(6)	
C3		4e	1		0.0564(7)	0.3823(12)	0.1964(10)	
H3A		4e	1		0.00910	0.42310	0.24930	0.0800
H3B		4e	1		0.06330	0.26780	0.21480	0.0800
C4		4e	1		0.0133(7)	0.4130(12)	0.0215(9)	
H4A		4e	1		0.06270	0.37760	-0.02980	0.0750
H4B		4e	1		-0.04730	0.34830	-0.01770	0.0750
N1		4e	1		0.2989(5)	0.5135(7)	0.4936(8)	
H1A		4e	1		0.34480	0.47050	0.45300	0.0760
H1B		4e	1		0.31950	0.50290	0.59620	0.0760
H1C		4e	1		0.29160	0.61710	0.46920	0.0760
C1		4e	1		0.2004(7)	0.4306(12)	0.4311(10)	
H1D		4e	1		0.20960	0.31620	0.44870	0.0840
H1E		4e	1		0.15260	0.46810	0.48460	0.0840
C2		4e	1		0.1594(7)	0.4620(12)	0.2634(10)	
H2A		4e	1		0.20670	0.42200	0.21020	0.0770
H2B		4e	1		0.15260	0.57680	0.24610	0.0770

Table S3. Atomic parameters for $HdPbI_4$ obtained from single crystallography characterization.

Atom	Ox.	Wyck.	Site	S.O.F.	x/a	y/b	z/c	U [Å²]
Pb1		2a	-1		1.00000	0	1.00000	
I2		4e	1		0.95026(3)	0.19209(4)	0.67949(4)	
I1		4e	1		0.72611(3)	-0.08058(5)	0.92281(5)	
C1		4e	1		0.5385(6)	-0.0187(7)	0.4494(8)	
H1A		4e	1		0.49070	-0.06920	0.35530	0.0390
H1B		4e	1		0.59930	-0.09320	0.50300	0.0390
N1		4e	1		0.7605(6)	-0.0106(6)	0.3332(10)	
H1C		4e	1		0.81620	0.03200	0.41190	0.0650
H1D		4e	1		0.78980	-0.02750	0.25430	0.0650
H1E		4e	1		0.73690	-0.10210	0.36310	0.0650
C2		4e	1		0.5977(6)	0.1275(7)	0.4063(8)	
H2A		4e	1		0.53830	0.20950	0.37130	0.0450
H2B		4e	1		0.65620	0.16640	0.49860	0.0450
C3		4e	1		0.6570(6)	0.1003(8)	0.2832(8)	
H3A		4e	1		0.68400	0.20100	0.25460	0.0520
H3B		4e	1		0.59960	0.05720	0.19210	0.0520

Table S4. Atomic parameters for $BdPbI_4$ obtained from single crystallography characterization.

Atom	Ox.	Wyck.	Site	S.O.F.	x/a	y/b	z/c	U [Å^2]
Pb1		1a	1		0.55166(13)	0.51679(9)	0.99283(8)	
I6		1a	1		0.76845(18)	0.22772(14)	0.93489(11)	
I5		1a	1		0.48344(18)	0.40280(14)	1.29928(11)	
I1		1a	1		0.33467(19)	0.80439(13)	1.05101(11)	
I4		1a	1		0.62009(19)	0.63023(14)	0.68668(11)	
Pb2		1a	1		1.05214(13)	0.01639(9)	0.99273(8)	
I3		1a	1		0.21718(17)	0.30601(13)	1.04819(11)	
I2		1a	1		0.88576(17)	0.72680(13)	0.93925(11)	
I8		1a	1		0.83791(18)	-0.09556(14)	1.29750(11)	
I7		1a	1		1.26589(18)	0.12735(15)	0.68910(11)	
C3		1a	1		0.794(4)	0.2382(17)	0.5541(19)	
H3A		1a	1		0.68890	0.24450	0.53780	0.0750
H3B		1a	1		0.78930	0.30210	0.61490	0.0750
C6		1a	1		0.299(2)	0.793(2)	0.4429(16)	
H6A		1a	1		0.31980	0.73290	0.37720	0.0560
H6B		1a	1		0.38770	0.77710	0.47950	0.0560
C5		1a	1		0.303(3)	0.964(2)	0.3790(16)	
H5A		1a	1		0.20410	0.98280	0.35420	0.0540
H5B		1a	1		0.29960	1.02590	0.44100	0.0540
C7		1a	1		0.1332(18)	0.738(2)	0.5483(17)	
H7A		1a	1		0.04350	0.75560	0.51290	0.0510
H7B		1a	1		0.11360	0.79410	0.61640	0.0510
C2		1a	1		0.928(5)	0.3003(19)	0.4349(18)	
H2A		1a	1		0.90940	0.24950	0.37220	0.1360
H2B		1a	1		1.02810	0.25910	0.44890	0.1360
C4		1a	1		0.809(3)	0.066(2)	0.6199(19)	
H4A		1a	1		0.82320	0.00200	0.55780	0.0640
H4B		1a	1		0.90750	0.05980	0.64570	0.0640
C8		1a	1		0.135(3)	0.5622(18)	0.6060(16)	
H8A		1a	1		0.02010	0.51510	0.64570	0.0500
H8B		1a	1		0.19580	0.51260	0.53630	0.0500
C1		1a	1		0.983(5)	0.475(2)	0.358(2)	
H1A		1a	1		0.94670	0.54220	0.41840	0.0920
H1B		1a	1		1.10480	0.48910	0.31760	0.0920
N2		1a	1		0.656(3)	0.008(2)	0.7365(13)	
H2C		1a	1		0.65620	0.05190	0.80060	0.0850
H2D		1a	1		0.65400	-0.09460	0.76310	0.0850
H2E		1a	1		0.56480	0.03290	0.71600	0.0850
N3		1a	1		0.449(2)	1.0093(16)	0.2677(17)	
H3C		1a	1		0.53050	1.04260	0.29040	0.0730
H3D		1a	1		0.42770	1.08570	0.20940	0.0730

H3E	1a	1	0.48090	0.92840	0.23260	0.0730
N4	1a	1	0.211(3)	0.538(2)	0.699(2)	
H4C	1a	1	0.21730	0.62670	0.72330	0.0930
H4D	1a	1	0.31400	0.50830	0.66560	0.0930
H4E	1a	1	0.14990	0.46510	0.76890	0.0930
N1	1a	1	0.905(2)	0.5168(17)	0.2552(12)	
H1C	1a	1	0.96780	0.48590	0.18420	0.0630
H1D	1a	1	0.89960	0.61950	0.23450	0.0630
H1E	1a	1	0.80170	0.47000	0.28560	0.0630

Table S5. Mean value and standard deviation (STDEV) of short-circuit current density, open-circuit voltage, fill factor, and power conversion efficiency for 5 solar cells fabricated with $BdAPbI_4$ absorber.

	Eff (%)	Voc (V)	Jsc (mAcm-2)	FF
1	1.082	0.87	2.894	0.43
2	1.016	0.82	2.753	0.45
3	0.936	0.88	2.801	0.38
4	0.974	0.85	2.592	0.442
5	0.845	0.78	2.702	0.401
Average±STDEV	0.971±0.089	0.84±0.041	2.75±0.112	0.421±0.029

Table S6. Mean value and standard deviation (STDEV) of short-circuit current density, open-circuit voltage, fill factor, and power conversion efficiency for 5 solar cells fabricated with $HdAPbI_4$ absorber.

	Eff (%)	Voc (V)	Jsc (mAcm-2)	FF
1	0.592	0.725	1.735	0.471
2	0.532	0.715	1.65	0.451
3	0.536	0.702	1.55	0.493
4	0.445	0.602	1.45	0.51
5	0.383	0.552	1.506	0.461
Average±STDEV	0.497±0.083	0.659±0.077	1.578±0.114	0.477±0.024

Table S7. Mean value and standard deviation (STDEV) of short-circuit current density, open-circuit voltage, fill factor, and power conversion efficiency for 5 solar cells fabricated with $OdAPbI_4$ absorber.

	Eff (%)	Voc (V)	Jsc (mAcm-2)	FF
1	0.012	0.732	0.047	0.340
2	0.007	0.720	0.031	0.302
3	0.008	0.652	0.035	0.37
4	0.006	0.551	0.029	0.407
5	0.003	0.593	0.016	0.287
Average±STDEV	0.0072±0.0032	0.649±0.078	0.031±0.011	0.341±0.049

Table S8. Mean value and standard deviation (STDEV) of short-circuit current density, open-circuit voltage, fill factor, and power conversion efficiency for 5 solar cells fabricated with $MAPbI_3$ light absorber.

	Eff (%)	Voc (V)	Jsc (mAcm-2)	FF
1	2.117	0.805	5.858	0.449
2	2.098	0.81	5.607	0.462
3	1.900	0.760	5.816	0.430
4	2.049	0.723	6.032	0.470
5	2.091	0.790	5.504	0.481
Average±STDEV	2.051±0.088	0.777±0.036	5.763±0.209	0.458±0.020

Table S9. IV characteristics data after 48 hours and 96 hours.

	Eff (%)	Voc (V)	Jsc (mAcm-2)	FF
$BdAPbI_4$(after 48 H)	0.866	0.88	2.425	0.406
$BdAPbI_4$(after 96 H)	0.798	0.85	2.29	0.410
$HdAPbI_4$(after 48 H)	0.454	0.715	1.405	0.452
$HdAPbI_4$(after 96 H)	0.339	0.69	1.26	0.39
$MAPbI_3$(after 48 H)	0.37	0.715	1.208	0.431
$MAPbI_3$(after 96 H)	0.028	0.69	0.112	0.36

Table S10. Maximum valence band position obtained from Cyclic Voltammetry and Ultraviolet Photoelectron Spectroscopy.

	VB position from CV (eV)	VB position from UPS (eV)
$BdAPbI_4$	-5.33	-5.38
$HdAPbI_4$	-5.59	-5.64
$OdAPbI_4$	-5.36	-5.55

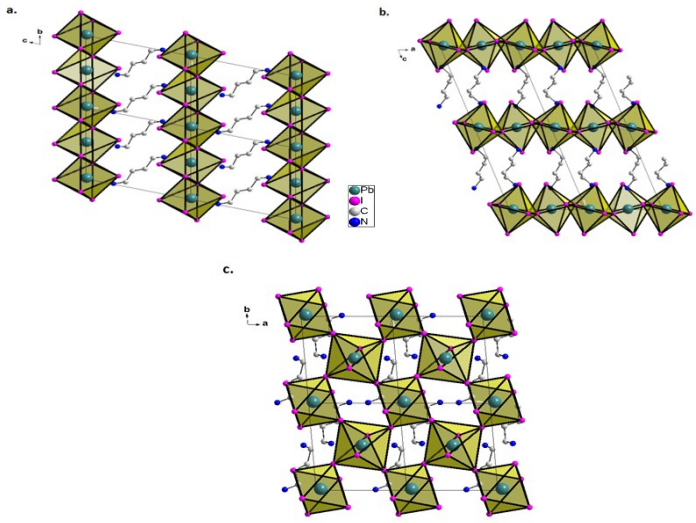

Figure S1.Structure of BdAPbI4 showed in Ball and stick model in 3 different axes. Single crystals were obtained from gently decreasing temperature of a concentrated aqueous solution. Characterization was performed at room temperature.

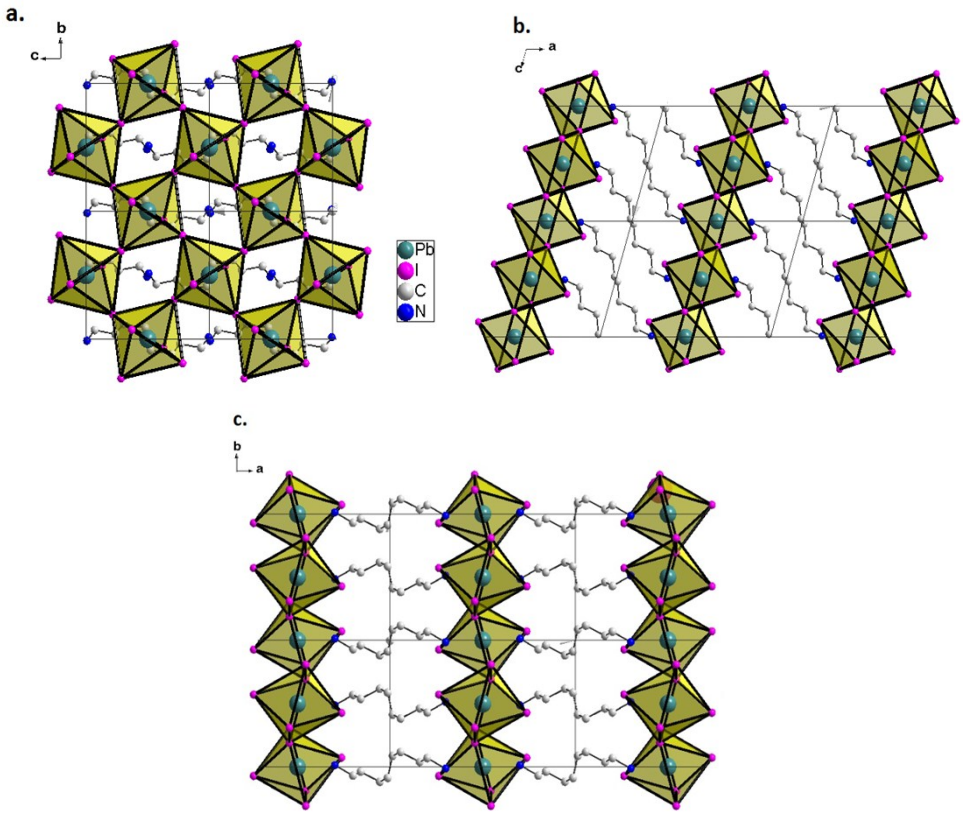

Figure S2. Structure of $OdAPbI_4$ showed in Ball and stick model in 3 different axes. Single crystals were obtained from gently decreasing temperature of a concentrated aqueous solution. Characterization was performed at room temperature.

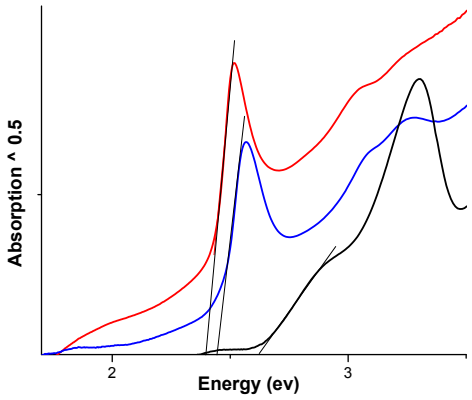

Figure S3. Tauc plots of --- $BdAPbI_4$,--- $HdAPbI_4$, and --- $OdAPbI_4$

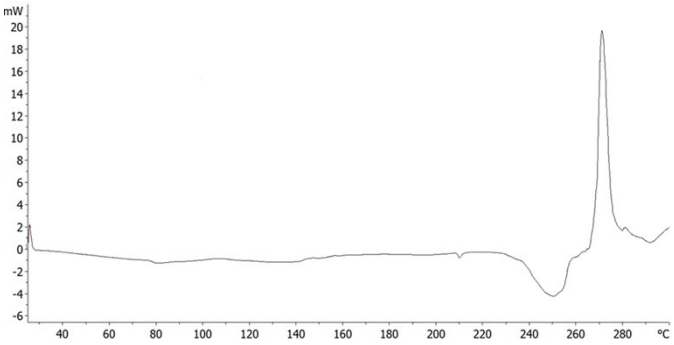

Figure S4. DSC graph of $BdAPbI_4$.

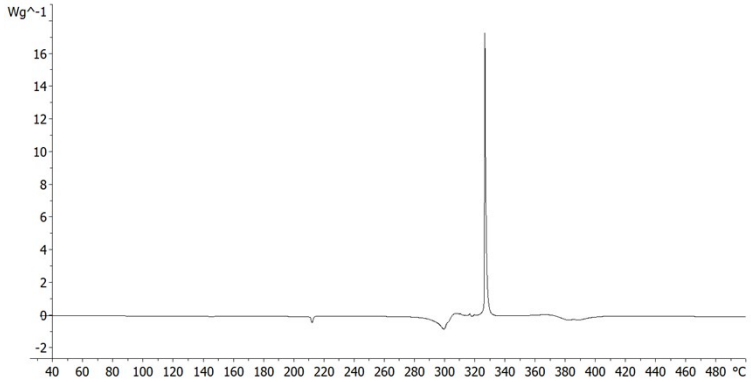

Figure S5. DSC graph of $HdAPbI_4$.

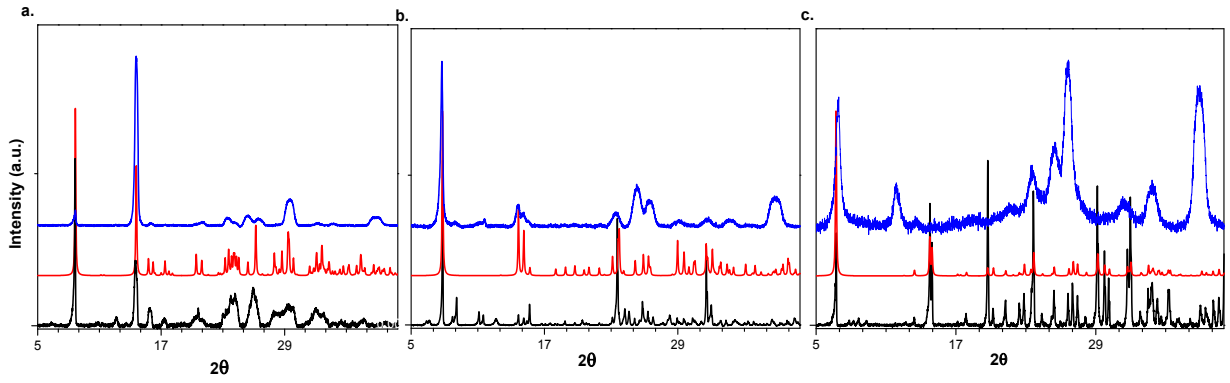

Figure S6. XRD patterns of a. $BdAPbI_4$, b. $HdAPbI_4$ and c. $OdAPbI_4$ presented as --- powder sample, --- calculated pattern from single crystal data and --- spin coated sample on mesoporous TiO_2 for assembly of solar cells.

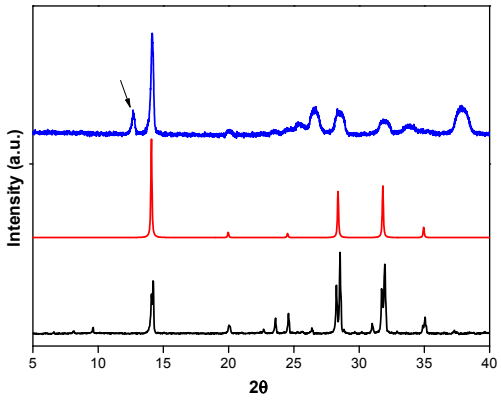

Figure S7. Comparison of $MAPbI_3$ XRD patterns, --- tetragonal phase powder sample at room temperature [1], --- calculated powder pattern from cubic single crystal data[1] , and --- spin coated sample at ambient atmosphere on mesoporous TiO_2 for fabrication of solar cells. The pattern shows peaks of PbI_2 indicating the instability of $MAPbI_3$ at ambient atmosphere.

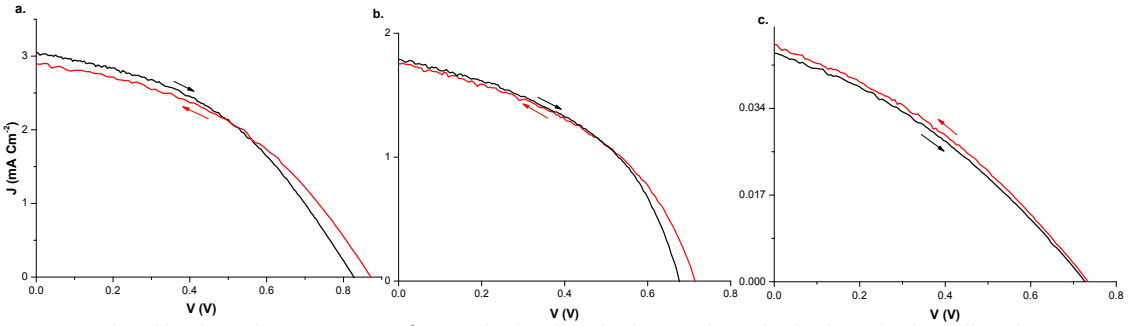

Figure S8. Forward and backward measurement for a. $BdAPbI_4$, b. $HdAPbI_4$, and c. $OdAPbI_4$ based solar cells indicating small hysteresis.

Table S11. IV characteristics for solar cells measured at 10mV/s scan rate. Bias voltage is scanned from Voc to 0 in the red values, and for the black ones from 0 to Voc.

	Jsc (mA cm^{-2})	V (V)	FF	η (%)
$BdAPbI_4$	2.894	0.870	0.430	1.082
	3.054	0.825	0.424	1.069
$HdAPbI_4$	1.735	0.725	0.471	0.592
	1.789	0.675	0.459	0.554
$OdAPbI_4$	0.047	0.732	0.34	0.012
	0.045	0.726	0.34	0.011

Figure S9. Representative photographs of spin coated material's film on TiO_2 substrates for fabrication of solar cells and XRD characterization.

References

1. Safdari, M.; Fischer, A.; Xu, B.; Kloo, L.; Gardner, J. M., Structure and function relationships in alkylammonium lead(ii) iodide solar cells. *Journal of Materials Chemistry A* 2015, 3, (17), 9201-9207.